Tailoring Photoisomerization Pathways in Donor-Acceptor Stenhouse Adducts: The Role of the Hydroxy Group

Tailoring Photoisomerization Pathways in Donor-Acceptor Stenhouse Adducts: The Role of the Hydroxyl Group

Michael M. Lerch[†,], Miroslav Medved'[1,2], Andrea Lapini[‖,§], Adèle D. Laurent[3], Alessandro Iagatti[‖,&,], Laura Bussotti[‖], Wiktor Szymański[‡,†], Wybren Jan Buma[4], Paolo Foggi[‖,&,⊥], Mariangela Di Donato[‖,&,*], Ben L. Feringa[†,*]

† Centre for Systems Chemistry, Stratingh Institute for Chemistry, University of Groningen, Nijenborgh 4, 9747 AG, Groningen, The Netherlands
‡ Department of Radiology, University of Groningen, University Medical Center Groningen, Hanzeplein 1, 9713 GZ, Groningen, The Netherlands
‖ LENS (European Laboratory for Non Linear Spectroscopy), via N. Carrara 1, 50019 Sesto Fiorentino, Italy
& INO (Istituto Nazionale di Ottica), Largo Fermi 6, 50125 Firenze, Italy
§ Dipartimento di Chimica "Ugo Schiff", Università di Firenze, via della Lastruccia 13, 50019 Sesto Fiorentino, Italy
⊥ Dipartimento di Chimica, Università di Perugia, via Elce di Sotto 8, 06100 Perugia, Italy
1 Regional Centre of Advanced Technologies and Materials, Department of Physical Chemistry, Faculty of Science, Palacký University in Olomouc, 17. listopadu 1192/12, CZ-771 46 Olomouc, Czech Republic
2 Department of Chemistry, Faculty of Natural Sciences, Matej Bel University, Tajovského 40, SK-97400 Banská Bystrica, Slovak Republic
3 CEISAM, UMR CNRS 6230, BP 92208, 2 Rue de la Houssinière, 44322 Nantes, Cedex 3, France
4 Van't Hoff Institute for Molecular Sciences, University of Amsterdam, Science Park 904, 1098XH Amsterdam, The Netherlands

Keywords: *photoswitching, donor-acceptor Stenhouse adducts, (mero)cyanine, hydroxy group, electronic effects, photoswitching mechanism, time-resolved spectroscopy, TD-DFT, NMR in situ-irradiation*

Abstract: Donor acceptor Stenhouse adducts (DASAs) are a rapidly emerging class of visible light-activatable negative photochromes. They are closely related to (mero)cyanine dyes with the sole difference being a hydroxy group in the polyene chain. The presence or absence of the hydroxy group has far-reaching consequences for the photochemistry of the compound: cyanine dyes are widely used as fluorescent probes, whereas DASAs hold great promise for visible-light-triggered photoswitching. Here we analyze the photophysical properties of a DASA lacking the hydroxy group. Ultrafast time-resolved pump-probe spectroscopy in both the visible and IR region show the occurrence of *E-Z* photo-isomerization on a 20 ps timescale, revoking familiarities with the photochemical behavior of DASAs, but on a slower time-scale. In contrast to the parent DASA compounds, where the initial photo-isomerization is constrained to a single position (next to the hydroxy group), ^{1}H-NMR *in situ*-irradiation studies at 213 K reveal that for non-hydroxy DASAs *E-Z* photo-isomerization can take place at two different bonds, yielding two distinct isomers. These observations are supported by TD-DFT calculations, showing that in the excited state the hydroxy group (pre)selects the neighboring C_2-C_3 bond for isomerization. The TD-DFT analysis also explains the larger solvatochromic shift observed for the parent DASAs as compared to the non-hydroxy analogue, in terms of the dipole moment changes evoked upon excitation. Furthermore, computations provide helpful insights into the photoswitching energetics, indicating that without the hydroxy group the 4π-electrocyclization step is energetically forbidden. Our results establish the central role of the hydroxy group for DASA photoswitching and suggest that its introduction allows for tailoring photo-isomerization pathways, presumably both through (steric) fixation *via* a hydrogen bond with the adjacent carbonyl group of the acceptor moiety, as well as through electronic effects on the polyene backbone. These insights are essential for the rational design of novel, improved DASA photoswitches and for a better understanding of the properties of both DASAs and cyanine dyes.

Introduction

Polymethine dyes, and more specifically cyanine dyes (Figure 1a),[1] have been used for a plethora of applications, such as materials[2,3] and chemosensing,[4] and continue to be essential for modern cellular biology.[5-7] Hallmarks of this structurally highly diverse class of photochromic molecules include high extinction coefficients, high fluorescence quantum yields and photostability. Since their introduction, they have been used for photography based on silver halides and in optical discs.[2] More recently – together with other fluorescent dyes – they have had a profound impact on cellular biology as labels and fluorescent probes.[8,9] Merocyanines (Figure 1a) have additional properties, including a pronounced

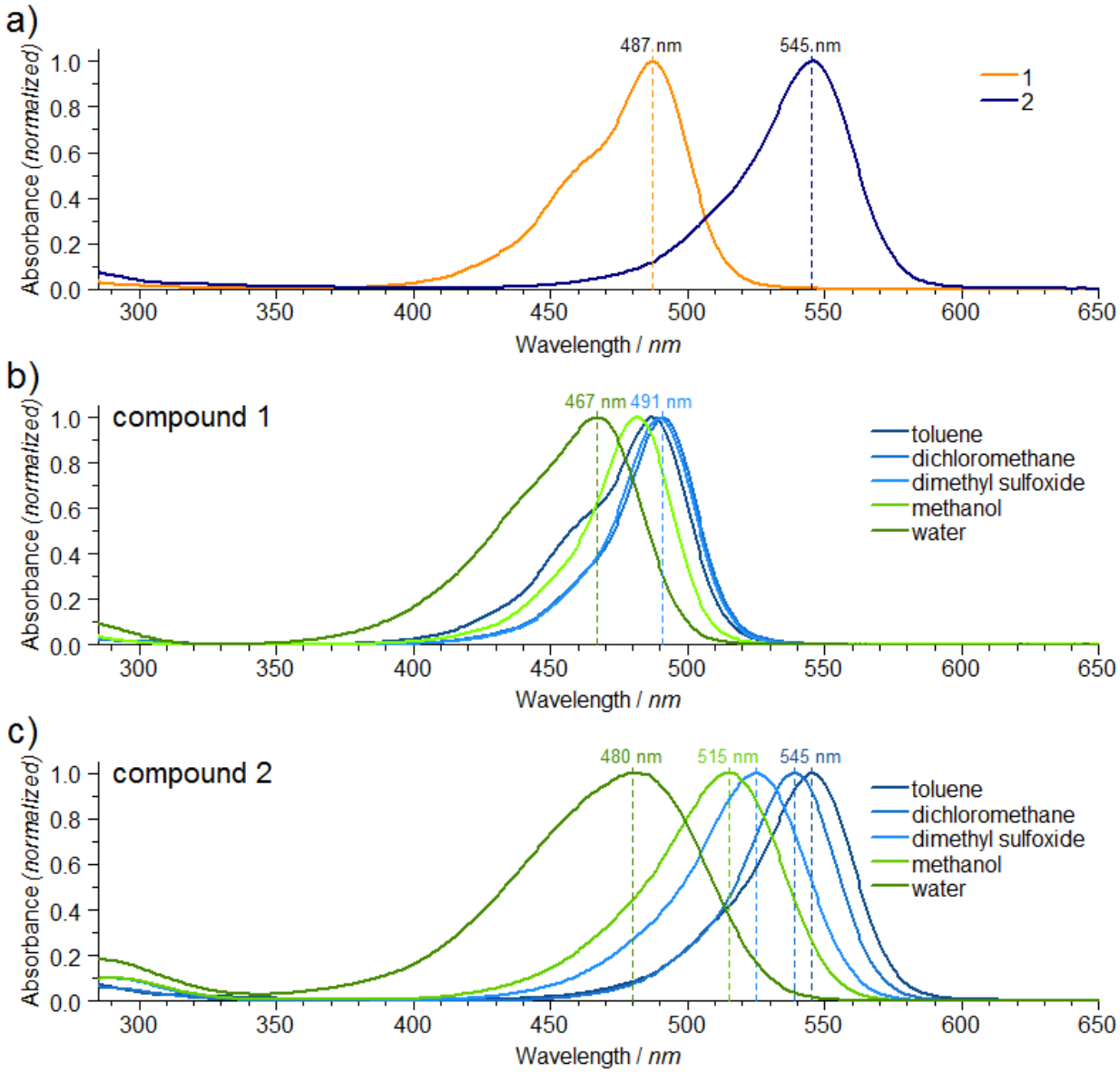

Figure 2: Comparison of UV/vis absorption spectra of compound **1** and **2** in different solvents: a) compound **1** and **2** in toluene; b) solvatochromism of compound **1** and c) solvatochromism of compound **2**.

Compared to the spectra of the parent DASA compound **2** (Figure 2c), the absorption band of compound **1** (Figure 2b) undergoes a hypsochromic shift in all solvents, indicating that the removal of the hydroxy functional group increases the gap between the HOMO and LUMO orbitals involved in the S_0-S_1 transition, which are mainly localized on the conjugated triene chain (see Figure 3a and b). The observed shifts are in good agreement with theoretical values (*e.g.* -0.27 eV *vs.* -0.36 eV for toluene; table S8.2) obtained by the TD-M06-2X method[46] using the 6-311++G(2df,2p) basis set[47] in combination with the universal continuum solvation model based on solute electron density (SMD)[48] and the corrected linear response (cLR) approach[49] to account for the solvent effects on both ground state (GS) and excited state (ES) electron densities. A red shift of the absorption as a function of polarity is observed among the investigated non-protic solvents, while the absorption band appears notably blue shifted in protic media such as water and methanol. The presence of the protic group in **2** leads to a generally stronger solvatochromism (Figure 2c). The observed trends are again well reproduced by the cLR/SMD/TD-DFT calculations (table S8.2). In particular, the stronger solvatochromism of **2** can be rationalized in terms of the changes of the dipole moment upon excitation. Whereas for **1** the change is almost negligible (0.29 D in chloroform) leading to very small solvatochromic shifts, for **2** it is noticeably larger and negative (-1.16 D in chloroform). Consequently, the more polar the solvent is, the more stabilized the GS becomes compared to the ES, leading to larger hypsochromic shifts.

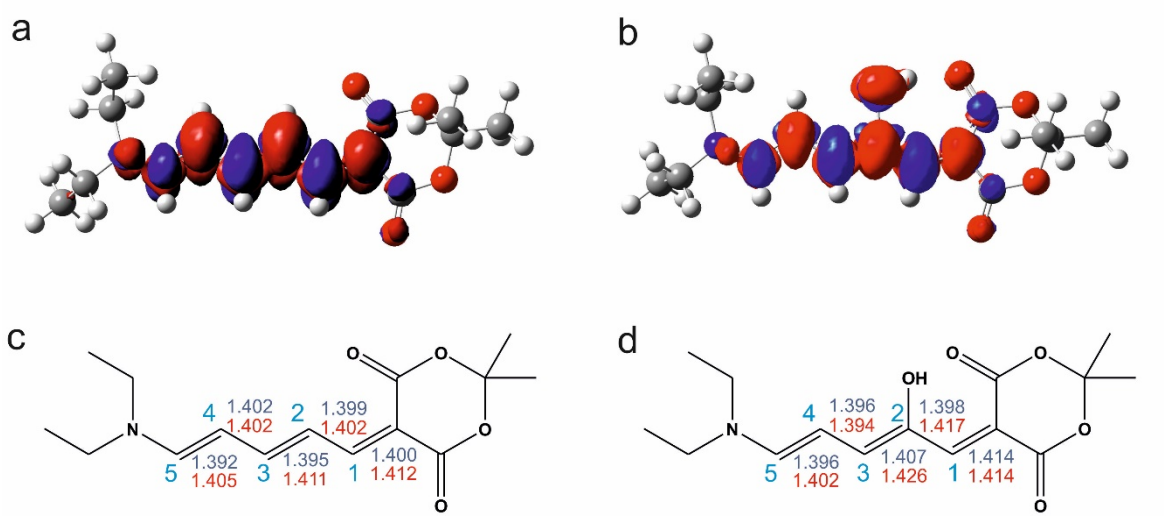

Figure 3: Electronic density difference (EDD) plots between the ES and the GS of **A** for compounds **1** (a) and **2** (b) in chloroform obtained at the SMD/M06-2X/6-311++G(2df,2p) level of theory. The blue (red) regions correspond to decrease (increase) in electron density upon electronic transition. A contour threshold of 0.001 a.u. has been applied. Bond lengths (in Å) are depicted for GS (blue) and ES (red) structures of the **A** form for **1** (c) and **2** (d) in chloroform. GS and ES geometries correspond to geometries optimized at the SMD/B3LYP/6-31++G(d,p) and SMD/TD-M06-2X/6-31+G(d) levels of theory, respectively.

The FTIR spectrum of compound **1** is reported in Figure 4, where the spectrum of **2** is also shown for comparison. Furthermore, Figure 4 reports the simulated FTIR spectra for both molecules obtained at the SMD/B3LYP/6-31++G(d,p) level using the harmonic approximation (FWHM = 12 cm^{-1}; scaling factor 0.98, SI section 8.2). It can be seen that spectra computed for **A** of both **1** and **2** satisfactorily reproduce all main features of the measured spectra, confirming that both molecules in the ground state attain a similar elongated triene conformation (SI section 8.1). Analysis of mode composition, as obtained by DFT, suggests that the differences between the FTIR spectra of **1** and **2**, in the reported frequency region, mainly arise from a different character of the C-C bonds along the conjugated chain, which is affected by the presence of a hydroxy group, and from the possibility to form a hydrogen bond between the hydroxy group and the acceptor carbonyl group in **2**. Whereas in **1** the bond length alternation indicates efficient π-conjugation, in the case of **2** the $C_{(A)}$-C_1 (A=Acceptor) and C_2-C_3 bonds are noticeably longer (see Figure 3c). The weakening of these two bonds brings about a small red shift of the 1160 cm^{-1} peak, which mainly accounts for the C_1-C_2/C_2-C_3 asymmetric bond stretching (coupled with the C_4-C_5 stretching and C-H rocking), and also more pronounced shifts of the *ca.* 1350-1380 cm^{-1} and 1500 cm^{-1} bands associated predominantly with the $C_{(A)}$-C_1 stretching and $C_{(A)}$-C_1/C_1-C_2 asymmetric stretching modes, respectively. A significant increase of the intensity of a band at *ca.* 1500 cm^{-1} is also observed in the case of compound **1**.

Further differences are noted in the 1600-1700 cm^{-1} region: in particular, the band observed at 1623 cm^{-1} in **2** almost disappears, while a band at 1674 cm^{-1} appears in the spectrum of the non-hydroxy analogue **1**. Our previous DFT analysis of **2** showed that there is a strong H-bond between the OH group linked to the triene chain and one of the carbonyl groups of the acceptor ring.[31,36] ^{1}H-NMR spectroscopy confirms the facile exchangeability of this proton (SI section 4). The observed spectral changes in the carbonyl region suggest the assignment of the 1623 cm^{-1} band to the H-bonded ring carbonyl stretch in case of **2**, which, upon the removal of the hydrogen bond in **1**, blue-shifts to 1675 cm^{-1} indicating a very strong hydrogen bond. This assignment is further supported by the presence of a band at 1700 cm^{-1} in **2**, due to the second non H-bonded carbonyl. The occurrence of a strong H-bond interaction in DASAs is also evidenced by the inspection of the FTIR spectra of compounds **1** and **2** in the 2500-3500 cm^{-1} region, which show for **2** an OH-stretch band at *ca.* 2900 cm^{-1} (see Figure S4.1). As yet, this H-bond has not received extensive attention, but it is clear that it will have mechanistic implications as it will influence the proton transfer step to form the zwitterionic structure **B** shown in Figure 1b for the first generation DASA **2**. From this point of view, studies of DASA derivatives in which the strength of such a hydrogen bond can be modulated would be highly interesting.

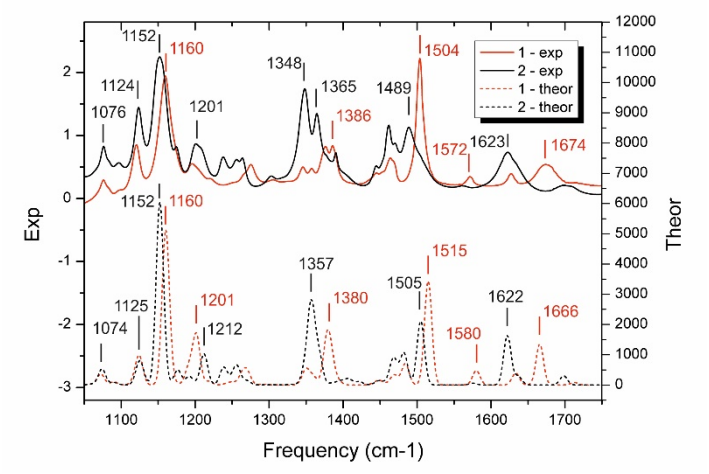

Figure 4: Comparison of the measured (upper) and simulated (lower) FTIR spectra of compound **1** (red line) and **2** (black line) in deuterated chloroform. For the computational details, see text.

To assess the usefulness of **1** as photoswitch, UV/vis spectroscopy with irradiation under steady-state conditions was performed (Figure 5, SI section 5). No photobleaching of the sample is observed upon irradiation as would be the case for **2**. However, a photostationary state is rapidly reached and maintained under irradiation. After irradiation is stopped, rapid relaxation is observed. A bathochromically shifted absorption band is temporarily apparent, reminiscent of the intermediate formed in the photoswitching of **2**.[33] Solvent-polarity influences the extent of this red-shift (SI section 5 and 7). Compound **1** shows clean photoswitching throughout a range of solvents (toluene, dichloromethane, chloroform, methanol, dimethyl sulfoxide, acetone, water and PBS buffer), with very little fatigue observed in aqueous environments.

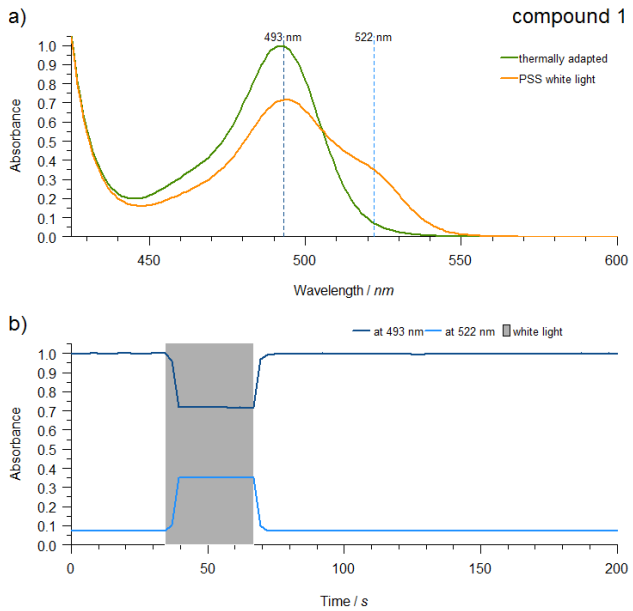

Figure 5: a) Absorption spectra for the photoisomerization of compound **1** (λ_{max} = 493 nm; ~6 µM in chloroform; 293 K) with white light (Thor-Labs, OSL1-EC, PSS = photostationary state) and b) corresponding time-evolution observed at 493 nm and 522 nm. The shaded area in grey indicates the irradiation period.

Time-resolved spectroscopy

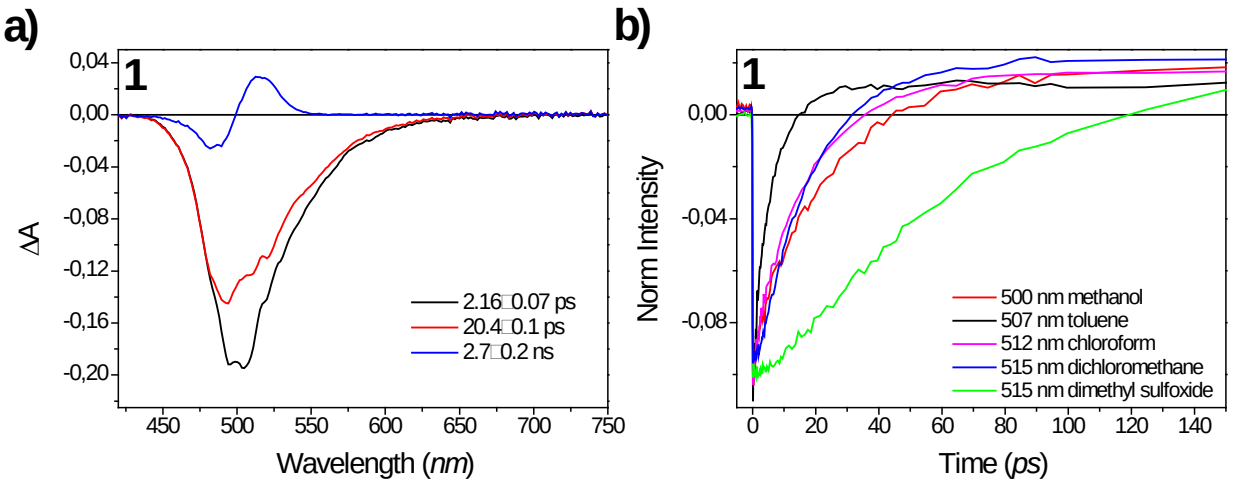

Figure 6: a) EADS obtained from global analysis[50] of time-resolved visible pump-probe data recorded for compound **1** dissolved in chloroform and excited at 480 nm; b) kinetic traces recorded on the maximum of the product band in various solvents.

Time-resolved spectroscopy allows detailed insights into the structure and dynamics of the compound in question during the actinic step. The EADS (Evolution-Associated Difference Spectra) obtained by global analysis[50] of visible pump-probe data recorded for compound **1** in chloroform upon λ = 480 nm light excitation (SI section 7) are shown in Figure 6. As evidenced from photo-accumulation experiments (Figure 5, SI section 5), the sample does not cyclize irrespective of the solvent. Nonetheless, a long-lived bathochromically shifted band peaking at 512 nm appears in the transient spectra *ca*. 20 ps after light absorption and it closely resembles that assigned to the *Z*-*E* isomerized intermediate (**A'**) observed in the parent DASA **2**.[33] The EADS shown in Figure 6 closely follow those reported for DASA **2**.[36] As noticed from inspection of Figure 6, in chloroform a bleaching band peaked at 500 nm, promptly appears upon photoexcitation. The signal intensity partially recovers in 2 ps, then, on a timescale of 20 ps, a positive band, peaking at 512 nm, appears in the transient spectra (see the blue EADS component reported in Figure 6a). The EADS obtained from transient absorption measurements repeated in different solvents are reported in the supporting information (Figure S7.1). The qualitative appearances of the transient signal and the observed spectral evolution do not significantly change when the solvent is modified. In all cases, a positive band peaking at 500-515 nm is observed in the long-lived spectral component. However, the maximum absorption band of the photoproduct and the observed shift with respect to the ground state absorption both depend on the solvent. This explains why in methanol, where the ground state absorption band is very broad, a bathochromically shifted band is hardly seen in steady-state photoaccumulation experiments (SI section 5.4). The quantum yields for the photoisomerization of **1** estimated from the ultrafast measurements are 10.7% (toluene), 16.2% (dichloromethane), 15.0% (chloroform), 14.3% (methanol) and 11.7% (dimethyl sulfoxide).
The dynamics of photoproduct formation is influenced by solvent polarity. A comparison of the kinetic traces recorded at the maximum absorption of the photogenerated species is reported in Figure 6b, showing that the rate of appearance of the positive peak in the transient spectra slows down upon increasing the polarity of the solvent. The time constant for the photoproduct formation is in fact 8.5 ps in toluene and increases up to 56 ps in dimethyl sulfoxide, where, besides a polarity effect, also the increased viscosity could play a role. It is, however, worth noticing that even in case of toluene the photoproduct is formed with a slower rate compared to the parent DASA molecule **2** (in that case the intermediate is observed on a 2 ps timescale) and no further spectral evolution of the product band is observed in any solvent.

To further characterize the nature of the photoproduct obtained upon light absorption for compound **1**, ps-transient infrared spectra were recorded. IR-based techniques are particularly suited to shed light on changes occurring in molecular structures upon photoexcitation and have been widely used to investigate light induced structural changes in polyene systems.[51-53] The EADS obtained from global analysis[50] of transient spectra acquired between 1100-1750 cm^{-1} are reported in Figure 7. In case of transient infrared measurements the sample has been excited on the red-edge of its absorption band, at 510 nm.

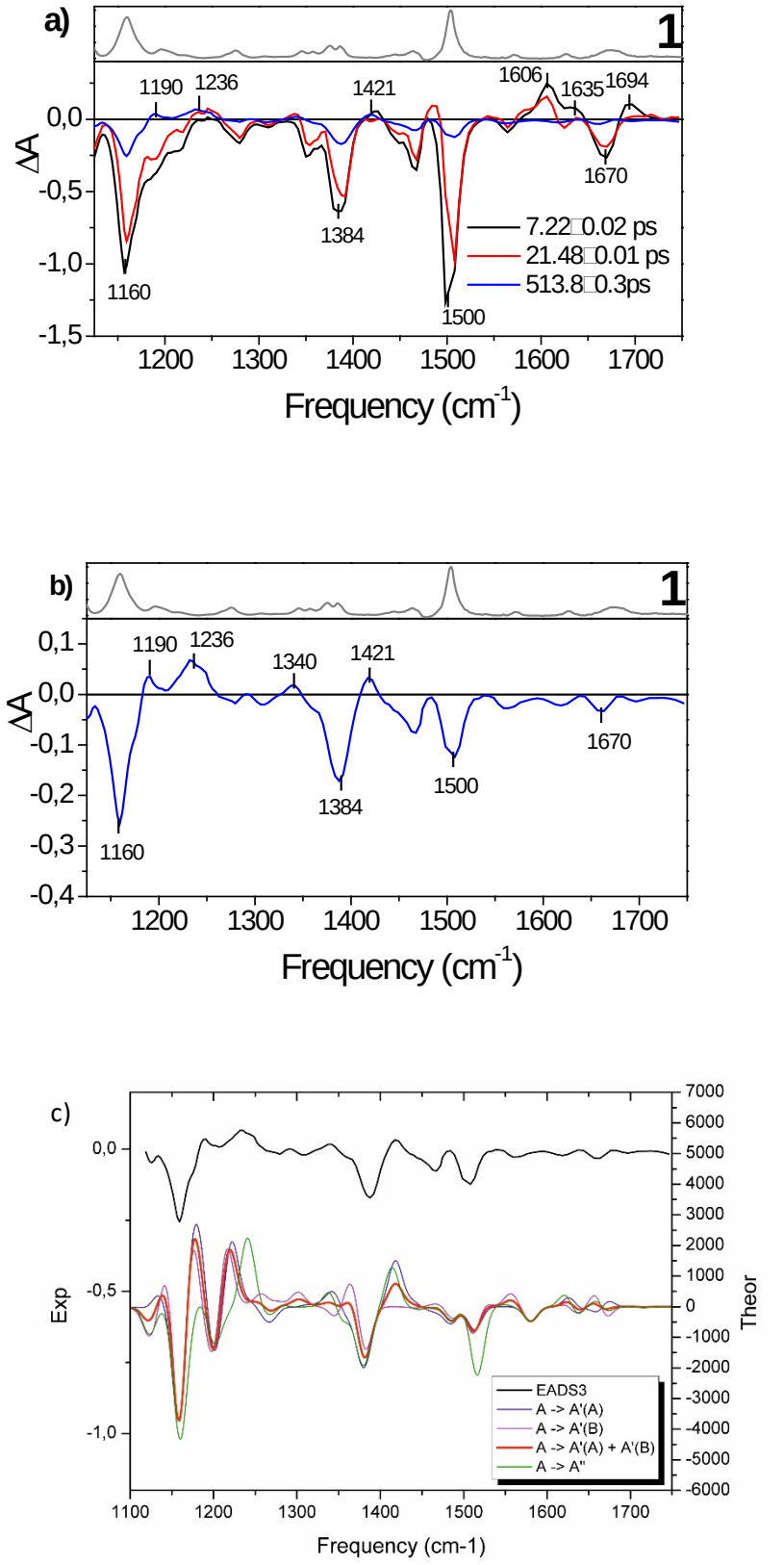

Figure 7: a) EADS obtained from global analysis[50] of time-resolved infrared data recorded for compound **1** in deuterated chloroform; the last spectral component is magnified in panel b). The gray line on the top panel of the figure reports the FTIR spectrum of the molecule in the same solvent. c) Comparison of experimental and simulated last EADS components in the same solvent. The blue/pink/red/green lines correspond to the GS difference harmonic IR spectra of the species

in the **B** form. The crossing point of the two curves enables us to estimate a barrier for intermolecular proton transfer (mediated by protic solvent). It can be seen that the barrier for the cyclization of compound **1** is very high (*ca.* 34 kcal/mol), which is related to very low acidity of the hydrogen atom bound to carbon (C_2). On the other hand, in the case of compound **2** the presence of the hydroxy group clearly facilitates the proton transfer decreasing the activation barrier to *ca.* 21 kcal/mol. Such a proton-transfer step is in so far important, as Stenhouse salts lacking such a strong hydrogen bond show strongly pH-dependent photoswitching.[43] In addition, as has been suggested before,[42] the initially formed oxyallyl cation (for the Piancatelli reaction) is stabilized by resonance through the electronegative oxygen atom. This is not possible for compound **1**, lacking the hydroxy group, thus majorly contributing to the observed higher barrier for cyclization of **1** as compared to **2**.

Conclusions

The presented experimental and theoretical analyses have elucidated the important role of the hydroxy substituent on the DASA photoswitching capacity, especially the actinic step. This group enables DASA photoswitching by restricting photo-isomerization of compound **2** towards the sole formation of isomer **A'(A)**. The "preselection" of bond C_2-C_3 is likely due to a decreased electron density and elongation of that particular bond (particularly in the ES). Notably, in case of the non-hydroxy analogue **1**, two isomers **A'(A)** and **A'(B)** are formed at low temperature under irradiation in photoaccumulation experiments as observed by NMR spectroscopy.

Time-resolved UV/vis and IR spectroscopy has provided spectroscopic insights into details and timescales of the isomerization pathway. They fully support the occurrence of an *E-Z* isomerization upon photoexcitation, and support the formation of two photoswitched isomers, although the similarity of the DFT-predicted IR spectra of **A'(A)** and **A'(B)** impedes an unambiguous distinction of the two isomers. The comparison of the photoisomerization kinetics of **1** and **2** shows that the non-hydroxy analogue **1** isomerizes about ten times slower than the parent DASA. The increased photoisomerization rate observed for compound **2** can be rationalized in terms of the influence that the hydroxyl substituent has on the triene bond length alternation and through steric effects. A somehow related effect has been previously observed in case of the rhodopsin chromophore, where the introduction of a methyl substituent accelerates the photoisomerization rate in solution.[54,55] Overall, our results show that by introducing a hydroxy group in the C_2-position of the polyene chain one can control photoswitching pathways and enable cyclization. The role of the strong hydrogen-bond in the proton transfer step leading to **B** in compound **2** is of considerable interest but needs further study.

The presented results are directly applicable for improvements of DASA photoswitching, and are important for acquiring a better understanding of the (photo)chemical properties of DASAs and cyanine dyes. One particularly attractive approach includes the substitution of the hydroxy group with other polar protic groups such as thiols and amines or polarizing groups such as halides, and varying the position of these groups. Such studies are presently being pursued.

ASSOCIATED CONTENT

Supporting Information.

Experimental procedures and characterization of compounds, UV/vis absorption spectra and photoswitching studies in different solvents, fluorescence spectra, FTIR spectra and ultrafast visible and Mid-IR spectroscopy; EADS (Evolution Associated Difference Spectra) obtained by global analysis; TD-DFT computations and NMR *in-situ* irradiation experiments (PDF).

AUTHOR INFORMATION

Corresponding Author

*didonato@lens.unifi.it

*b.l.feringa@rug.nl

Author Contributions

The manuscript was written through contributions of all authors. All authors have given approval to the final version of the manuscript.

ACKNOWLEDGMENT

The authors gratefully acknowledge financial support from Laserlab-Europe (LENS002289), the Ministry of Education, Culture and Science (Gravitation program 024.001.035), The Netherlands Organization for Scientific Research (NWO–CW, Top grant to B.L.F., VIDI grant no. 723.014.001 for W.S.), the European Research Council (Advanced Investigator

Grant, no. 227897 to B.L.F.) and the Royal Netherlands Academy of Arts and Sciences Science (KNAW). M.M. acknowledges the Czech Science Foundation (project no. 16-01618S), the Ministry of Education, Youth and Sports of the Czech Republic (grant LO1305) and the Grant Agency of the Slovak Republic (VEGA project No. 1/0737/17). This research used computational resources of 1) the GENCI-CINES/IDRIS, 2) CCIPL (Centre de Calcul Intensif des Pays de Loire), 3) a local Troy cluster, and 4) the HPCC of the Matej Bel University in Banska Bystrica by using the infrastructure acquired in projects ITMS 26230120002 and 26210120002 supported by the Research and Development Operational Programme funded by the ERDF. The Swiss Study Foundation is acknowledged for a fellowship to M.M.L. We thank P. van der Meulen for support with the temperature dependent NMR *in-situ* irradiation studies and T. Tiemersma-Wegman for ESI-MS analyses.

References:

(1) Shindy, H. A. Fundamentals in the Chemistry of Cyanine Dyes: A Review. *Dye. Pigment.* **2017**, *145*, 505–513.
(2) Mishra, A.; Behera, R. K.; Behera, P. K.; Mishra, B. K.; Behera, G. B. Cyanines during the 1990s: A Review. *Chem. Rev.* **2000**, *100* (6), 1973–2011.
(3) Fabian, J.; Nakazumi, H.; Matsuoka, M. Near-Infrared Absorbing Dyes. *Chem. Rev.* **1992**, *92* (6), 1197–1226.
(4) Sun, W.; Guo, S.; Hu, C.; Fan, J.; Peng, X. Recent Development of Chemosensors Based on Cyanine Platforms. *Chem. Rev.* **2016**, *116* (14), 7768–7817.
(5) Strekowski, L.; Handa, H. *Heterocyclic Polymethine Dyes*; Strekowski, L., Ed.; Topics in Heterocyclic Chemistry; Springer: Berlin, Heidelberg, 2008; Vol. 14.
(6) Guo, Z.; Park, S.; Yoon, J.; Shin, I. Recent Progress in the Development of near-Infrared Fluorescent Probes for Bioimaging Applications. *Chem. Soc. Rev.* **2014**, *43* (1), 16–29.
(7) Lavis, L. D.; Raines, R. T. Bright Building Blocks for Chemical Biology. *ACS Chem. Biol.* **2014**, *9* (4), 855–866.
(8) Sameiro, M.; Gonçalves, T. Fluorescent Labeling of Biomolecules with Organic Probes. *Chem. Rev.* **2009**, *109* (1), 190–212.
(9) Wiederschain, G. Y. *The Molecular Probes Handbook. A Guide to Fluorescent Probes and Labeling Technologies*, 11th ed.; Johnson, I. D., Spence, M. T. Z., Eds.; Life technologies corporation, 2011; Vol. 76.
(10) Kulinich, A. V; Ishchenko, A. A. Merocyanine Dyes: Synthesis, Structure, Properties and Applications. *Russ. Chem. Rev.* **2009**, *78* (2), 141–164.
(11) Dempsey, G. T.; Bates, M.; Kowtoniuk, W. E.; Liu, D. R.; Tsien, R. Y.; Zhuang, X. Photoswitching Mechanism of Cyanine Dyes. *J. Am. Chem. Soc.* **2009**, *131* (51), 18192–18193.
(12) Vaughan, J. C.; Dempsey, G. T.; Sun, E.; Zhuang, X. Phosphine Quenching of Cyanine Dyes as a Versatile Tool for Fluorescence Microscopy. *J. Am. Chem. Soc.* **2013**, *135* (4), 1197–1200.
(13) Aramendia, P. F.; Krieg, M.; Nitsch, C.; Bittersmann, E.; Braslavsky, S. E. The Photophysics of Merocyanine 540. a Comparative Study in Ethanol and in Liposomes. *Photochem. Photobiol.* **1988**, *48* (2), 187–194.
(14) Benniston, A. C.; Harriman, A.; Gulliya, K. S. Photophysical Properties of Merocyanine 540 Derivatives. *J. Chem. Soc. Faraday Trans.* **1994**, *90* (7), 953.
(15) Le Guennic, B.; Jacquemin, D. Taking Up the Cyanine Challenge with Quantum Tools. *Acc. Chem. Res.* **2015**, *48* (3), 530–537.
(16) Vladimir A. Azov, D. F. *Molecular Switches*, 2nd Editio.; Feringa, B. L., Browne, W. R., Eds.; Wiley-VCH: Weinheim; Germany, 2011.
(17) Brieke, C.; Rohrbach, F.; Gottschalk, A.; Mayer, G.; Heckel, A. Light-Controlled Tools. *Angew. Chemie - Int. Ed.* **2012**, *51* (34), 8446–8476.
(18) Russew, M. M.; Hecht, S. Photoswitches: From Molecules to Materials. *Adv. Mater.* **2010**, *22* (31), 3348–3360.
(19) de Silva, A. P. *Molecular Logic-Based Computation, Monographs in Supramolecular Chemistry*; RSC Publishing, 2012.
(20) Klajn, R. Spiropyran-Based Dynamic Materials. *Chem. Soc. Rev.* **2014**, *43* (1), 148–184.
(21) Natali, M.; Giordani, S. Molecular Switches as Photocontrollable "smart" Receptors. *Chem. Soc. Rev.* **2012**, *41* (10), 4010.
(22) Szymański, W.; Beierle, J. M.; Kistemaker, H. A. V.; Velema, W. A.; Feringa, B. L. Reversible Photocontrol of Biological Systems by the Incorporation of Molecular Photoswitches. *Chem. Rev.* **2013**, *113* (8), 6114–6178.
(23) Velema, W. A.; Szymanski, W.; Feringa, B. L. Photopharmacology: Beyond Proof of Principle. *J. Am. Chem. Soc.* **2014**, *136* (6), 2178–2191.
(24) Broichhagen, J.; Frank, J. A.; Trauner, D. A Roadmap to Success in Photopharmacology. *Acc. Chem. Res.* **2015**, *48* (7), 1947–1960.
(25) Erbas-Cakmak, S.; Leigh, D. A.; McTernan, C. T.; Nussbaumer, A. L. Artificial Molecular Machines. *Chem. Rev.* **2015**, *115* (18), 10081–10206.
(26) Yun, C.; You, J.; Kim, J.; Huh, J.; Kim, E. Photochromic Fluorescence Switching from Diarylethenes and Its Applications. *J. Photochem. Photobiol. C Photochem. Rev.* **2009**, *10* (3), 111–129.
(27) Irie, M.; Fukaminato, T.; Sasaki, T.; Tamai, N.; Kawai, T. Organic Chemistry: A Digital Fluorescent Molecular Photoswitch. *Nature* **2002**, *420* (6917), 759–760.
(28) Helmy, S.; Leibfarth, F. A.; Oh, S.; Poelma, J. E.; Hawker, C. J.; De Alaniz, J. R. Photoswitching Using Visible Light: A New Class of Organic Photochromic Molecules. *J. Am. Chem. Soc.* **2014**, *136* (23), 8169–8172.
(29) Helmy, S.; Oh, S.; Leibfarth, F. A.; Hawker, C. J.; Read De Alaniz, J. Design and Synthesis of Donor-Acceptor Stenhouse Adducts: A Visible Light Photoswitch Derived from Furfural. *J. Org. Chem.* **2014**, *79* (23), 11316–11329.
(30) Lerch, M. M.; Hansen, M. J.; Velema, W. A.; Szymanski, W.; Feringa, B. L. Orthogonal Photoswitching in a Multifunctional Molecular System. *Nat. Commun.* **2016**, *7*, 12054.
(31) Laurent, A. D.; Medved', M.; Jacquemin, D. Using Time-Dependent Density Functional Theory to Probe the Nature of Donor–Acceptor Stenhouse Adduct Photochromes. *ChemPhysChem* **2016**, *17* (12), 1846–1851.
(32) Belhboub, A.; Boucher, F.; Jacquemin, D. An Ab Initio Investigation of Photoswitches Adsorbed onto Metal Oxide

Surfaces: The Case of Donor–acceptor Stenhouse Adduct Photochromes on TiO_2 Anatase. *J. Mater. Chem. C* **2017**, *5* (7), 1624–1631.

(33) Lerch, M. M.; Wezenberg, S. J.; Szymanski, W.; Feringa, B. L. Unraveling the Photoswitching Mechanism in Donor-Acceptor Stenhouse Adducts. *J. Am. Chem. Soc.* **2016**, *138* (20), 6344–6347.

(34) Hemmer, J. R.; Poelma, S. O.; Treat, N.; Page, Z. A.; Dolinski, N. D.; Diaz, Y. J.; Tomlinson, W.; Clark, K. D.; Hooper, J. P.; Hawker, C.; et al. Tunable Visible and Near Infrared Photoswitches. *J. Am. Chem. Soc.* **2016**, *138* (42), 13960–13966.

(35) Mallo, N.; Brown, P. T.; Iranmanesh, H.; MacDonald, T. S. C.; Teusner, M. J.; Harper, J. B.; Ball, G. E.; Beves, J. E. Photochromic Switching Behaviour of Donor–acceptor Stenhouse Adducts in Organic Solvents. *Chem. Commun.* **2016**, *52* (93), 13576–13579.

(36) Di Donato, M.; Lerch, M. M.; Lapini, A.; Laurent, A. D.; Iagatti, A.; Bussotti, L.; Ihrig, S. P.; Medved', M.; Jacquemin, D.; Szymanski, W.; et al. Shedding Light on the Photo-Isomerization Pathway of Donor–Acceptor Stenhouse Adducts. *J. Am. Chem. Soc.* **2017**, *just accep.*

(37) Piancatelli, G.; Scettri, A.; Barbadoro, S. A Useful Preparation of 4-Substituted 5-Hydroxy-3-Oxocyclopentene. *Tetrahedron Lett.* **1976**, *17* (39), 3555–3558.

(38) Palmer, L. I.; De Alaniz, J. R. Rapid and Stereoselective Synthesis of Spirocyclic Ethers via the Intramolecular Piancatelli Rearrangement. *Org. Lett.* **2013**, *15* (3), 476–479.

(39) Veits, G. K.; Wenz, D. R.; Read De Alaniz, J. Versatile Method for the Synthesis of 4-Aminocyclopentenones: Dysprosium(III) Triflate Catalyzed Aza-Piancatelli Rearrangement. *Angew. Chemie - Int. Ed.* **2010**, *49* (49), 9484–9487.

(40) Palmer, L. I.; Read De Alaniz, J. Direct and Highly Diastereoselective Synthesis of Azaspirocycles by a dysprosium(III) Triflate Catalyzed Aza-Piancatelli Rearrangement. *Angew. Chemie - Int. Ed.* **2011**, *50* (31), 7167–7170.

(41) Riveira, M. J.; Marsili, L. A.; Mischne, M. P. The Iso-Nazarov Reaction. *Org. Biomol. Chem.* **2017**.

(42) Nieto Faza, O.; Silva López, C.; Álvarez, R.; De Lera, Á. R. Theoretical Study of the Electrocyclic Ring Closure of Hydroxypentadienyl Cations. *Chem. - A Eur. J.* **2004**, *10* (17), 4324–4333.

(43) Honda, K.; Komizu, H.; Kawasaki, M. Reverse Photocharomism of Stenhouse Salts. *J. Chem. Soc. Chem. Commun.* **1982**, No. 4, 253.

(44) McNab, H.; Monahan, L. C.; Gray, T. Thermal Cyclisation Reactions of Vinylogous Aminomethylene Meldrum's Acid Derivatives. *J. Chem. Soc. Chem. Commun.* **1987**, *0* (3), 140.

(45) Yang, S.; Liu, J.; Cao, Z.; Li, M.; Luo, Q.; Qu, D. Fluorescent Photochromic Donor-Acceptor Stenhouse Adduct Controlled by Visible Light. *Dye. Pigment.* **2018**, *148*, 341–347.

(46) Zhao, Y.; Truhlar, D. G. The M06 Suite of Density Functionals for Main Group Thermochemistry, Thermochemical Kinetics, Noncovalent Interactions, Excited States, and Transition Elements: Two New Functionals and Systematic Testing of Four M06-Class Functionals and 12 Other Function. *Theor. Chem. Acc.* **2008**, *120* (1–3), 215–241.

(47) Ditchfield, R.; Hehre, W. J.; Pople, J. A. Self-Consistent Molecular-Orbital Methods. IX. An Extended Gaussian-Type Basis for Molecular-Orbital Studies of Organic Molecules. *J. Chem. Phys.* **1971**, *54* (2), 724–728.

(48) Marenich, A. V.; Cramer, C. J.; Truhlar, D. G. Universal Solvation Model Based on Solute Electron Density and on a Continuum Model of the Solvent Defined by the Bulk Dielectric Constant and Atomic Surface Tensions. *J. Phys. Chem. B* **2009**, *113* (18), 6378–6396.

(49) Caricato, M.; Mennucci, B.; Tomasi, J.; Ingrosso, F.; Cammi, R.; Corni, S.; Scalmani, G. Formation and Relaxation of Excited States in Solution: A New Time Dependent Polarizable Continuum Model Based on Time Dependent Density Functional Theory. *J. Chem. Phys.* **2006**, *124* (12), 124520.

(50) Van Stokkum, I. H. M.; Larsen, D. S.; Van Grondelle, R. Global and Target Analysis of Time-Resolved Spectra. *Biochim. Biophys. Acta - Bioenerg.* **2004**, *1657* (2–3), 82–104.

(51) Di Donato, M.; Ragnoni, E.; Lapini, A.; Foggi, P.; Hiller, R. G.; Righini, R. Femtosecond Transient Infrared and Stimulated Raman Spectroscopy Shed Light on the Relaxation Mechanisms of Photo-Excited Peridinin. *J. Chem. Phys.* **2015**, *142* (21), 212409.

(52) Ragnoni, E.; Di Donato, M.; Iagatti, A.; Lapini, A.; Righini, R. Mechanism of the Intramolecular Charge Transfer State Formation in All-Trans -β-Apo-8′-Carotenal: Influence of Solvent Polarity and Polarizability. *J. Phys. Chem. B* **2015**, *119* (2), 420–432.

(53) Kardas, T. M.; Ratajska-Gadomska, B.; Lapini, A.; Ragnoni, E.; Righini, R.; Di Donato, M.; Foggi, P.; Gadomski, W. Dynamics of the Time-Resolved Stimulated Raman Scattering Spectrum in Presence of Transient Vibronic Inversion of Population on the Example of Optically Excited Trans-β-Apo-8′-Carotenal. *J. Chem. Phys.* **2014**, *140* (20), 204312.

(54) Sovdat, T.; Bassolino, G.; Liebel, M.; Schnedermann, C.; Fletcher, S. P.; Kukura, P. Backbone Modification of Retinal Induces Protein-like Excited State Dynamics in Solution. *J. Am. Chem. Soc.* **2012**, *134* (20), 8318–8320.

(55) Demoulin, B.; Altavilla, S. F.; Rivalta, I.; Garavelli, M. Fine Tuning of Retinal Photoinduced Decay in Solution. *J. Phys. Chem. Lett.* **2017**, *8* (18), 4407–4412.

TOC Figure